The Abundant Histone Chaperones Spt6 and FACT Collaborate to Assemble, Inspect, and Maintain Chromatin Structure in *Saccharomyces cerevisiae*

Laura McCullough, Zaily Connell, Charisse Petersen, and Tim Formosa[1]

Department of Biochemistry, University of Utah School of Medicine, Salt Lake City, Utah 84112

ORCID ID: 0000-0002-8477-2483 (T.F.)

ABSTRACT *Saccharomyces cerevisiae* Spt6 protein is a conserved chromatin factor with several distinct functional domains, including a natively unstructured 30-residue N-terminal region that binds competitively with Spn1 or nucleosomes. To uncover physiological roles of these interactions, we isolated histone mutations that suppress defects caused by weakening Spt6:Spn1 binding with the *spt6-F249K* mutation. The strongest suppressor was H2A-N39K, which perturbs the point of contact between the two H2A-H2B dimers in an assembled nucleosome. Substantial suppression also was observed when the H2A-H2B interface with H3-H4 was altered, and many members of this class of mutations also suppressed a defect in another essential histone chaperone, FACT. Spt6 is best known as an H3-H4 chaperone, but we found that it binds with similar affinity to H2A-H2B or H3-H4. Like FACT, Spt6 is therefore capable of binding each of the individual components of a nucleosome, but unlike FACT, Spt6 did not produce endonuclease-sensitive reorganized nucleosomes and did not displace H2A-H2B dimers from nucleosomes. Spt6 and FACT therefore have distinct activities, but defects can be suppressed by overlapping histone mutations. We also found that Spt6 and FACT together are nearly as abundant as nucleosomes, with ~24,000 Spt6 molecules, ~42,000 FACT molecules, and ~75,000 nucleosomes per cell. Histone mutations that destabilize interfaces within nucleosomes therefore reveal multiple spatial regions that have both common and distinct roles in the functions of these two essential and abundant histone chaperones. We discuss these observations in terms of different potential roles for chaperones in both promoting the assembly of nucleosomes and monitoring their quality.

KEYWORDS histone chaperones; nucleosome reorganization; Spt6; FACT

SPT6 is a highly conserved factor implicated in several steps in gene expression, including initiation, elongation, and termination of transcription, as well as processing and export of messenger RNA (mRNA) and achieving appropriate post-translational modification of histones at actively transcribed sites (Compagnone-Post and Osley 1996; Hartzog *et al.* 1998; Endoh *et al.* 2004; Bucheli and Buratowski 2005; Kaplan *et al.* 2005; Yoh *et al.* 2007, 2008; Ardehali *et al.* 2009; Ivanovska *et al.* 2011; DeGennaro *et al.* 2013; Dronamraju and Strahl 2013). Spt6 has several known activities that are relevant for participating in this broad range of functions, including binding to RNA polymerase II, DNA, his-

tones, and nucleosomes (Bortvin and Winston 1996; Krogan *et al.* 2002; Yoh *et al.* 2007; McDonald *et al.* 2010; Close *et al.* 2011). One effect of diminished Spt6 function *in vivo* is decreased nucleosome occupancy in transcribed regions, resulting in inappropriate activation of transcription owing to loss of repressive chromatin (Kaplan *et al.* 2003; Adkins and Tyler 2006; Jamai *et al.* 2009; Hainer *et al.* 2011; Ivanovska *et al.* 2011; Thebault *et al.* 2011; DeGennaro *et al.* 2013; Kato *et al.* 2013a). Spt6 therefore both promotes the production and processing of appropriate RNAs and also prevents the production of inappropriate transcripts at least partly by maintaining chromatin in a repressive state. Current models suggest that Spt6 accomplishes this by binding to RNA polymerase II during transcription and then using its multiple functional domains to coordinate the activities of transcription elongation and mRNA processing machinery with the reassembly of chromatin after the passage of the polymerase (DeGennaro *et al.* 2013; Kato *et al.* 2013b).

The 1451-residue *Saccharomyces cerevisiae* Spt6 protein has at least three structural domains: a natively unstructured

~300-residue N-terminal region that is highly acidic (over one-third aspartate and glutamate residues, estimated $pK_i = \sim 4.0$), a central region of about 950 amino acids with multiple functional sequence motifs and overall similarity to the prokaryotic transcription factor *Tex* (Johnson *et al.* 2008), and an ~200-residue C-terminal region with both the known SH2 modules found in this yeast (the tandem SH2 domain) (Diebold *et al.* 2010b; Sun *et al.* 2010; Close *et al.* 2011). Spt6 binds directly to nucleosomes and to the transcription factor Spn1/Iws1 (Krogan *et al.* 2002; Lindstrom *et al.* 2003; Yoh *et al.* 2008; Zhang *et al.* 2008; Diebold *et al.* 2010a; McDonald *et al.* 2010). Remarkably, both interactions are mediated by the same 30-residue peptide within the unstructured N-terminal domain (Spt6$^{239-268}$). Binding is competitive because addition of Spn1 disrupts the interaction between Spt6 and nucleosomes, suggesting a switching mechanism in which the association of Spt6 with nucleosomes is regulated by Spn1 binding (McDonald *et al.* 2010). Mutations that weaken the Spt6:Spn1 interaction cause significant defects in transcriptional repression, and mutations that ablate binding are lethal (McDonald *et al.* 2010). Spt6$^{239-268}$ therefore has an important role in maintaining chromatin integrity, and this role appears to involve competition between binding of Spt6 to Spn1 or to nucleosomes, but the purpose of the Spt6:nucleosome interaction, its physiological context, and the function of the competition with Spn1 are unknown.

FACT is also an essential conserved factor that can bind free histones or assembled nucleosomes (Belotserkovskaya *et al.* 2004; Xin *et al.* 2009; Winkler *et al.* 2011). FACT also functions in a broad range of processes, in this case including transcription initiation and elongation and DNA replication (Belotserkovskaya *et al.* 2004; Winkler and Luger 2011; Formosa 2012). FACT has two subunits (Spt16-SSRP1 in higher eukaryotes and Spt16-Pob3 in yeasts and fungi), each with multiple structural and functional domains (VanDemark *et al.* 2006, 2008; Winkler and Luger 2011; Hondele *et al.* 2013; Kemble *et al.* 2013). Nucleosomes bound by FACT *in vitro* adopt a reorganized structure that retains all the components of the nucleosome but in a less compact configuration in which the DNA is more accessible to some restriction endonucleases and to RNA polymerase II and from which dissociation of H2A-H2B dimers becomes more probable (Xin *et al.* 2009; Formosa 2012; Hsieh *et al.* 2013). The ability to induce or trap this reorganized form and, conversely, to resolve loosely organized combinations of histones and DNA into canonical nucleosomes has been proposed to be the central function of FACT, allowing it to participate in both nucleosome disassembly and nucleosome assembly (Formosa 2012).

Genetic analysis of FACT has provided significant insight into the features and physiological functions of nucleosome reorganization (VanDemark *et al.* 2008; McCullough *et al.* 2011, 2013). Mutations in different domains of FACT cause distinct defects *in vivo* and *in vitro*, and mutations in histones can either compensate for decreased FACT activity or exacerbate the defects, with different FACT alleles producing different profiles of genetic interactions. For example, the nucleosome reorganization model suggests that H2A-H2B dimers must be dissociated from DNA and from (H3-H4)$_2$ tetramers. Consistent with this, the *spt16-11* mutation causes a defect in nucleosome reorganization activity *in vitro*, and both this and some of the phenotypic effects of this allele *in vivo* can be suppressed by mutations in H2A-H2B that weaken the interface between dimers and tetramers (McCullough *et al.* 2011). In contrast, these same histone mutations are neutral or detrimental when combined with the *pob3-Q308K* allele, affecting the small subunit of FACT, and the effects of this allele were instead suppressed by mutations that affect the flexibility of the H4 N-terminal domain junction region, whose conformation has been proposed to be important during nucleosome assembly (McCullough *et al.* 2013). Histone mutations therefore can provide a probe for the features of histones and nucleosomes that participate in the dynamic interactions among chaperones, histones, and nucleosomes.

To investigate how Spt6 interacts with histones and nucleosomes and how competition by Spn1 affects these interactions, we isolated histone mutants that suppress the phenotypes caused by weakening the Spt6:Spn1 interface. We reasoned that suppressor mutations might counteract the effects of diminished Spt6:Spn1 binding by weakening competing interactions or activities and therefore report on the function of the switch. We previously used the Spt6:Spn1 structure to design a set of mutations predicted to disturb this interaction and showed that the strength of the resulting phenotypes correlated with altered affinity (McDonald *et al.* 2010). The *spt6-F249K* allele was chosen for the studies reported here because it caused strong defects but retained adequate viability for genetic analysis. Our results show a surprising overlap between features of nucleosomes that affect the functions of Spt6 and those that affect FACT, but they also highlight unique activities of these two essential histone chaperones. *spt6-F249K* defects were partially suppressed by many of the same histone alleles that suppressed phenotypes caused by the *spt16-11* FACT mutation, suggesting that multiple histone chaperones benefit from promoting dissociation of H2A-H2B from (H3-H4)$_2$. However, the strongest suppression was observed with an H2A-N39K allele that alters the interface between the two H2A-H2B dimers in a nucleosome, and this mutation was not beneficial to FACT mutants. There are therefore different ways for a nucleosome to be unstable, and Spt6 and FACT differ regarding which internal features or spatial domains of the nucleosome are important for their respective activities.

Our results revealed that H2A-H2B dimer:dimer interactions are particularly important in cells lacking efficient Spt6:Spn1 binding, prompting us to examine whether Spt6 binds H2A-H2B directly. Immobilized Spt6 was previously reported to bind preferentially to H3-H4 (Bortvin and Winston 1996), but we found that in solution it has similar affinity for H2A-H2B and H3-H4. Spt6 and FACT are therefore both capable of binding each of the individual components of

nucleosomes as well as the assembled products, but Spt6 did not produce the increased accessibility to DNA associated with FACT-mediated nucleosome reorganization. We conclude that Spt6 and FACT have both overlapping and distinct functional interactions with histones and nucleosomes and that binding to each of the components of a nucleosome is not sufficient to produce nucleosome reorganization. To explain the distinct and overlapping effects of histone mutations on histone chaperone functions, we propose that the interaction between Spn1 and Spt6 has an important role in monitoring the quality of nucleosome assembly and the integrity of existing chromatin and that Spt6 and FACT are abundant chaperones that collaborate to assemble, inspect, and maintain chromatin.

Materials and Methods

Histone genes were mutagenized by standard PCR amplification, as described previously (McCullough *et al.* 2011, 2013). Briefly, a *spt6-F249K* strain with all eight genomic histone genes deleted was constructed with a *URA3*-marked low-copy-number plasmid carrying *HTA1-HTB1* and *HHT2-HHF2* as the only sources of histones. These histone genes and about 400 base pairs of flanking vector sequence were amplified from the plasmid by standard PCR using *Pfu* polymerase, the product was mixed with a linearized empty vector marked with *LEU2*, and the mixture was used to transform the *spt6-F249K* histone deletion strain. Leu$^+$ clones resulting from recombination between the PCR product and the linearized vector *in vivo* were replica plated to medium containing 5-FOA to select cells lacking the *URA3*-marked plasmid. Viable clones containing only PCR-mutagenized histone genes were screened for the ability to grow at elevated temperatures that are restrictive for *spt6-F249K* strains, plasmids were isolated from these clones and used to transform a fresh host strain to ensure linkage of the Ts$^-$ suppression with the histone mutation, and then the four histone genes on the plasmid were sequenced to identify suppressing mutations. Multiple independent PCR pools were used, and isolates with the same mutation were considered to be independent only if they came from different PCR reactions. A subset of the mutations identified was integrated into the genome at each of the two similar genes that encode each histone, resulting in strains expressing only the mutant histone alleles from endogenous loci with genetic markers downstream of each gene, as described previously (McCullough *et al.* 2011, 2013). Combinations of integrated mutations then were obtained by standard genetic crosses (Table 1).

Spt6 was purified from a bacterial expression system as described by Close *et al.* (2011). Fluorescence-labeled recombinant histones based on *S. cerevisiae* or *Xenopus laevis* histone sequences were assembled into nucleosomes using a 5S ribosomal DNA (rDNA) sequence, and then complex formation, rate of digestion by *Dra*I, and displacement of H2A-H2B dimers were assayed as described by Xin *et al.* (2009).

To measure protein abundance, cells were grown to logarithmic phase and harvested by centrifugation. Cell number was determined by hemacytometer counting, and proteins were extracted by the trichloroacetic acid (TCA) method, which provides significantly higher yields of these large proteins than the standard boiling SDS method used previously (VanDemark *et al.* 2008) (data not shown). Briefly, cells in log phase were collected by centrifugation, washed with water, and then suspended in 20% TCA. The cells were lysed by agitating with glass beads (eight cycles of 2 min at 4°) and then collected and washed with acetone. The cell fragments were suspended in 50 mM Tris-Cl (pH 7.5), 20 mM Tris base, and 2% SDS; boiled for 8 min; and debris was removed by centrifugation. The concentration of soluble proteins was determined using the Bio-Rad DC protein assay, and then 5–7 µg of total protein was separated by SDS-PAGE in parallel with purified target proteins. Proteins were detected using appropriate polyclonal antisera and infrared-labeled secondary antisera detected with an Odyssey scanner (LI-COR Biosciences). Only experiments with acceptable dose-response curves in which signals from all samples were flanked by standards were analyzed.

Data availability

Strains are available upon request. Supporting Information contains additional documentation of genetic interactions in Figure S1, Figure S2, and Figure S3.

Results

Histone mutations suppress phenotypes caused by spt6- F249K

To investigate the physiological functions supported by the nucleosome/Spn1-binding region of Spt6, we isolated histone mutations that diminish the temperature sensitivity caused by the *spt6-F249K* allele (Figure 1). Twenty-nine independent candidates with single mutations were identified; although H3 and H4 were available for mutation and an identical strategy revealed H3-H4 mutations in a search for suppressors of the FACT allele *pob3-Q308K* (McCullough *et al.* 2013), all 29 simple suppressors obtained were alleles of H2A or H2B. Seven of these were H2A-N39K mutants, and these also produced the highest overall suppression of phenotypes (Figure 1). Nine of the mutants affected H2B-A84, including conversion of this alanine to aspartate, valine, or threonine, with variable effects described later. H2B-A84D and -A84V also were recovered previously as suppressors of the *spt16-11* mutation in the large subunit of the histone chaperone FACT (McCullough *et al.* 2011), producing the surprising result that these two histone chaperone defects can be suppressed by the same change in H2A-H2B. Similarly, H2B-F68S and -Y86C were isolated in both screens (Figure 1, blue font). We therefore tested the other histone mutations that suppress defects caused by *spt16-11* and found that all had at least some ability to ameliorate the effects of *spt6-F249K* as well (Figure 1, green font). The converse was not true because some mutations isolated only in the *spt6-F249K* screen resulted in moderate suppression of *spt16-11* strains,
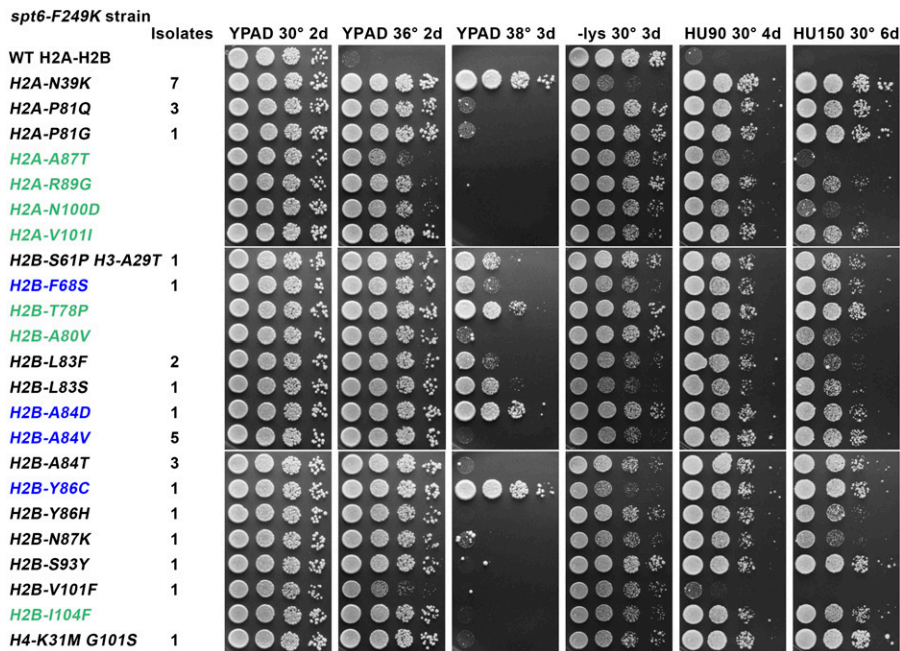
Figure 1 Histone mutations suppress phenotypes caused by *spt6-F249K*. Strain 8857-13-1 pTF237 (*spt6-F249K* lacking genomic histone genes) (see Table 1) was transformed with low-copy centromere plasmids carrying the *LEU2* marker and one copy of each histone gene with either the wild-type (WT) sequence or the mutation shown. After selecting for loss of the WT histone genes on pTF237, the strains were tested for growth under various conditions. Black font indicates mutations isolated only in the screen for suppressors of the temperature sensitivity caused by *spt6-F249K*, green indicates mutations isolated in a previous screen using an *spt16-11* strain (Mccullough *et al.* 2011) that were found to also suppress phenotypes caused by *spt6-F249K*, and blue indicates mutations isolated in both screens. The number of independent isolates with the same mutation from the *spt6-F249K* screen are indicated. Cultures were grown to saturation in rich medium, and then aliquots of 10-fold serial dilutions were placed on the plates indicated and incubated at the temperature shown for the time given in days. Growth on medium lacking lysine indicates the Spt⁻ phenotype in these strains with the *lys2-128∂* allele. HU indicates addition of hydroxyurea to YPAD (rich medium) at 90 or 150 mM.

but others were strongly detrimental (*e.g.*, H2B-L83S and -V101F) (Supporting Information, Figure S1A). These same histone mutations had minor effects in otherwise normal strains (Figure S1B) and were typically strongly detrimental or lethal in a strain with a mutation in the small subunit of FACT, *pob3-Q308K* (Figure S1C). Notably, the response to histone mutations was more similar for Spt16 and Spt6 than for Spt16 and Pob3, so domains of unrelated histone chaperones can have functional requirements more like one another than domains within the same histone chaperone complex.

In addition to the Ts⁻ phenotype, *spt6-F249K* also caused a strong Spt⁻ phenotype (Figure 1), monitored here as inappropriate expression of the normally inactive *lys2-128∂* reporter leading to a Lys⁺ growth phenotype (Simchen *et al.* 1984). Nucleosomes are a crucial component of genome-wide transcriptional repression (Kaplan *et al.* 2003; Hainer *et al.* 2011), so the Spt⁻ phenotype can be a sensitive measurement of global chromatin integrity. Alterations in the expression levels or sequences of histone genes can lead to abnormal chromatin production and therefore can cause the Spt⁻ phenotype (Clark-Adams *et al.* 1988), and several of the histone mutations identified here cause mild or moderate effects on their own (Figure S1B). Remarkably, some of the histone mutations reduce the Spt⁻ phenotype caused by *spt6-F249K*, especially H2A-N39K (Figure 1), a mutation that does not cause this phenotype itself (Figure S1B). H2A-N39K and a subset of the other histone mutations therefore appear to restore chromatin integrity in *spt6-F249K* strains.

A third effect of the *spt6-F249K* mutation is severe sensitivity to the replication toxin hydroxyurea (HU) (Figure 1).

Screens for HU sensitivity (HUs) have yielded mutations in a variety of processes (Hartman and Tippery 2004), including transcription elongation factors such as the PAF1 complex (Betz *et al.* 2002), but it is not yet obvious how a phenotype more typically associated with DNA replication and repair is related to these transcription functions. Our screen required only suppression of the Ts⁻ phenotype caused by *spt6-F249K*, but the histone mutations we identified also suppressed the HUs phenotype, except in the case of the weakest suppressor, H2B-V101F (Figure 1). The unselected cosuppression of the Ts⁻ and HUs phenotypes suggests that both phenotypes result from the same fundamental defect in Spt6 function. The correlation is not perfect; *e.g.*, H2A-P81Q is among the strongest suppressors of the HUs phenotype but is among the weaker suppressors of the Ts⁻ phenotype (Figure 1), and H2B-A84D produced stronger suppression of the Ts⁻ phenotype than H2B-A84T or -A84V, but all three substitutions at this residue caused similar suppression of the HUs phenotype. The stresses caused by elevated temperature and exposure to HU in a *spt6-F249K* mutant therefore appear to be closely related but not identical.

Together these results show that *spt6-F249K* compromises several processes, including the ability to grow at elevated temperatures, the ability to maintain chromatin-based repression, and the ability to tolerate the replication toxin HU. Mutations in histones can ameliorate these defects to different extents, suggesting that these phenotypes result from a defect in the histone chaperone activity of Spt6. The overlapping suppression with some alleles of FACT but detrimental effects with others indicates that each chaperone domain relies on
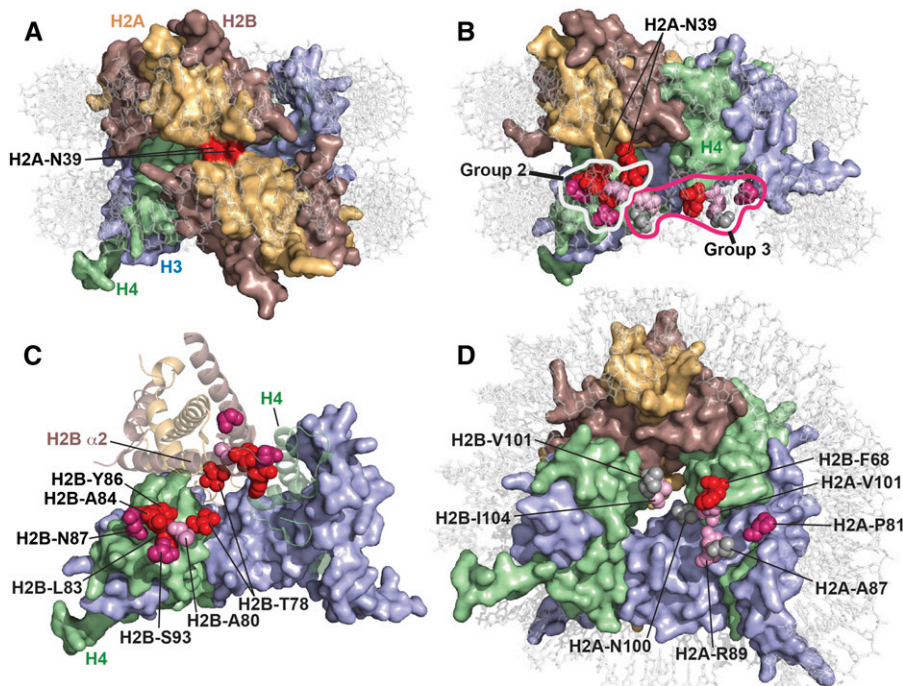
Figure 2 Physical environments of the suppressor mutations reveal spatial domains of nucleosomes important for Spt6 function. Residues mutated in *spt6-F249K* suppressors were mapped to the yeast nucleosome structure (PDB 1ID3) (White *et al.* 2001) using PyMol (Schrodinger). (A) Top view of a nucleosome with both H2A-N39 residues in surface mode colored red. (B) As in A, except rotated to the left, with one H2A-H2B dimer removed and the H2A-N39 residue in the remaining dimer colored the same as the rest of the protein. The residues affected by suppressor mutations are shown as spheres for the missing copy of the dimer only, to allow them to be seen because they are otherwise buried within the structure. The first group of suppressors is comprised entirely of H2A-N39K, and the second and third groups are described in the text and here. Suppressors were scored for their effects on growth rate, temperature sensitivity, HUs, and Spt⁻ phenotype in a *spt6-F249K* strain (see Figure 1), and the affected residues are color-coded here according to the aggregate score with red > purple > pink > gray. (C) A top view of the nucleosome is shown with the DNA removed to allow better visibility and the core proteins rotated slightly back into the plane of view. Both H3 molecules are shown in surface represen-

tation, one H4 is also a surface, while the other H4 molecule and one H2A-H2B dimer are rendered as ribbons, and the other H2A-H2B dimer is removed. The residues in Group 2 are identified for both H2A-H2B dimers and coded as in B. The residues in the front dimer are labeled and are shown nestling into the H4 surface. The residues in the back dimer are shown on the ribbon representation to highlight their clustering along and at the end of H2B helix α₂. H2A-N39 is removed for clarity; it lies above and between the H2B-T78 residues. (D) A nucleosomal face is shown with Group 3 residues identified and colored as earlier. This group represents several environments and contains mostly weaker suppressors. The exception, H2B-F68, is strong and makes direct contact with the H4 surface.

different but related functional properties of histones or nucleosomes when performing individual functions.

Suppressor mutations map to different regions within the nucleosome structure

The residues affected by the suppressor mutations represent at least three distinct environments within the nucleosome (Figure 2). The most common and strongest overall suppressor, H2A-N39K, occupies a particularly noteworthy location because this residue forms the major interface between the two H2A-H2B dimers within a nucleosome (White *et al.* 2001) (Figure 2A). While H2A-N39K strongly suppressed all the defects observed for *spt6-F249K*, it had little effect in normal strains or those with FACT mutations (weakly suppressive with *spt16-11*, moderately detrimental with *pob3-Q308K*) (Figure S1). The H2A-N39K mutation therefore reveals a specific functional feature or spatial domain of nucleosomes that is particularly relevant in cells with the *spt6-F249K* allele.

A second major group of residues affected by suppressor mutations is a cluster at the C-terminal end of the α₂-helix of H2B, where it makes extensive contact with H4 (Figure 2, B and C, Group 2). This set includes alterations of H2B-T78, -A80, -L83, -A84, -Y86, -N87, and -S93, including many of the mutations that were identified in both the *spt6-F249K* and *spt16-11* screens (Figure 1). H2B-T78 and -S93 are not as closely associated with the end of H2B-α₂ as the others, but they are likely to affect the position (S93Y) or stability (T78P)

of this long α-helix. The third group of mutations represents mostly weaker suppressors but also interrupts H2A-H2B dimer contact with H4 (Figure 2, B and D, Group 3). This group includes H2A-P81, -A87, and -R89 (residues that contact each other and abut H4, where H2A-α₃ and H2B-α₂ meet) (Figure 2D). The strong suppressor H2B-F68S alters a residue that directly contacts H4-Y98, and the weaker suppressors in H2B-V101 and -I104 also affect residues that make or support interactions with H4.

The common theme among the second and third groups of suppressor mutations is that they would be expected to destabilize the interface between H2A-H2B and H3-H4, especially the interface with H4. Consistent with this interpretation, we previously showed that nucleosomes assembled *in vitro* with H2B-A84D or H2A-V101I mutations are more likely than normal to lose H2A-H2B dimers when challenged with high temperatures or high-ionic-strength conditions (McCullough *et al.* 2011). While there are exceptions (*e.g.*, H2B-L83F/S directly contacts H4-Y72 and is in a cluster of residues expected or known to affect dimer retention but strongly suppresses only *spt6-F249K*), the general result is therefore that destabilizing the H2A-H2B interface with H4 is beneficial to both *spt6-F249K* and *spt16-11* mutants.

Effects of integrated histone mutations

Our previous studies showed that plasmid-based expression of histone genes does not fully recapitulate the effects of
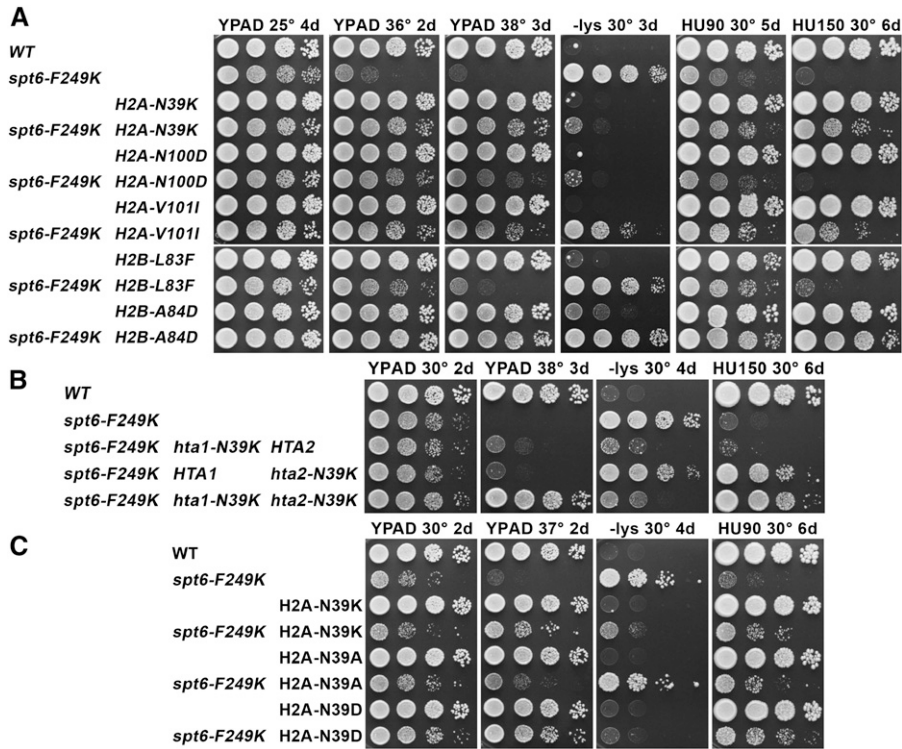
Figure 3 Effects of a subset of histone mutations after integration into both genomic copies of the genes. The mutations shown were integrated into *HTA1* and *HTA2* or into *HTB1* and *HTB2* along with a genetic marker downstream of the ORF, as indicated previously (McCullough *et al.* 2011). Standard genetic crosses were performed to combine the histone mutations with one another and with the *spt6* alleles indicated. The nomenclature used is "H2A-N39K" indicates a *hta1-N39K hta2-N39K* double mutant. (A) The effects of combining *spt6-F249K* with a subset of the histone mutations. (B) The effects of combining the *spt6-F249K* allele with normal and N39K-mutated versions (genetically marked in both cases) of *HTA1* and *HTA2*. (C) The effects of replacing H2A-N39 with a basic, neutral, or acidic residue.

mutations when they are expressed from a more native genomic context (McCullough *et al.* 2011, 2013). This may reflect increased flexibility in gene copy number that is possible with centromere-containing plasmids *vs.* chromosomes or differences in the expression patterns of the two similar copies of each histone gene (Feser *et al.* 2010; Eriksson *et al.* 2012; Kurat *et al.* 2014). We therefore integrated a subset of the histone mutations into both genomic copies of the relevant histone genes to test for effects with *spt6-F249K* (Figure 3A). In general, the profiles of suppression when mutations were integrated at both endogenous loci were similar to those observed using plasmid-based expression, with integration providing slightly stronger suppression in some cases. For example, H2A-N100D expressed from a low-copy plasmid did not permit growth at 38° and suppressed the Spt⁻ phenotype weakly, but stronger effects were observed on integration (compare Figure 1 to Figure 3A). The differences between plasmid-based and genomic expression also could be affected by a change in genetic background between the screen (W303 strain) and the integrated mutations (A364a strains).

This approach also allowed us to test the effects of mixed expression, in which only one copy of the histone gene was mutated. This revealed more significant differences between the two histone genes, especially with the effects of H2A-N39K. This mutation caused little or no effect in otherwise normal strains, whether *HTA1*, *HTA2*, or both were mutated (Figure 3, A and B). However, in a *spt6-F249K* strain, the Spt⁻ phenotype was strongly suppressed in *hta1-N39K hta2-N39K* and *hta1-N39K HTA2* strains but not in *HTA1 hta2-N39K* (Figure 3B). *HTA1* is essential for viability (Formosa *et al.*

2002) and was the gene used as the plasmid-borne source of H2A in the suppressor screen, so this result could simply reflect the reported higher expression of *HTA1* relative to *HTA2* (Feser *et al.* 2010). However, suppression of the Ts⁻ phenotype appeared to be additive, with equal contributions from *HTA1* and *HTA2*, and only the status of *HTA2* was important for suppression of the HUs phenotype because an *hta1-N39K HTA2* strain was sensitive, but *HTA1 hta2-N39K* was as resistant as *hta1-N39K hta2-N39K* (Figure 3B). The level of suppression produced by the H2A-N39K mutation therefore varies with both the source of the protein and the phenotype being tested. *HTA1* and *HTA2* produce slightly different proteins (residues 124 and 125 are ...AT... in *HTA1* and ...TA... in *HTA2*), and *HTA2-HTB2* lacks some forms of repression that affect the other six histone genes (Eriksson *et al.* 2012; Kurat *et al.* 2014). Little is known about differential regulation of the two genes under different stress conditions or the consequences of forming hybrid nucleosomes with normal and mutant proteins, but these results indicate that these can be important considerations and that plasmid-based expression of histone mutations can mask significant features of histone gene expression.

The primary contact between the two H2A-H2B dimers in a yeast nucleosome is through the two H2A-N39 side chains (Figure 2) (White *et al.* 2001). Complementarity of the dipole moments of these residues makes a small contribution to the overall stability of the nucleosome, but insertion of two positively charged lysine residues into this constrained space is expected to destabilize the nucleosome structure locally as a result of charge repulsion. If this repulsion is the source of the suppression observed with the H2A-N39K mutation, then
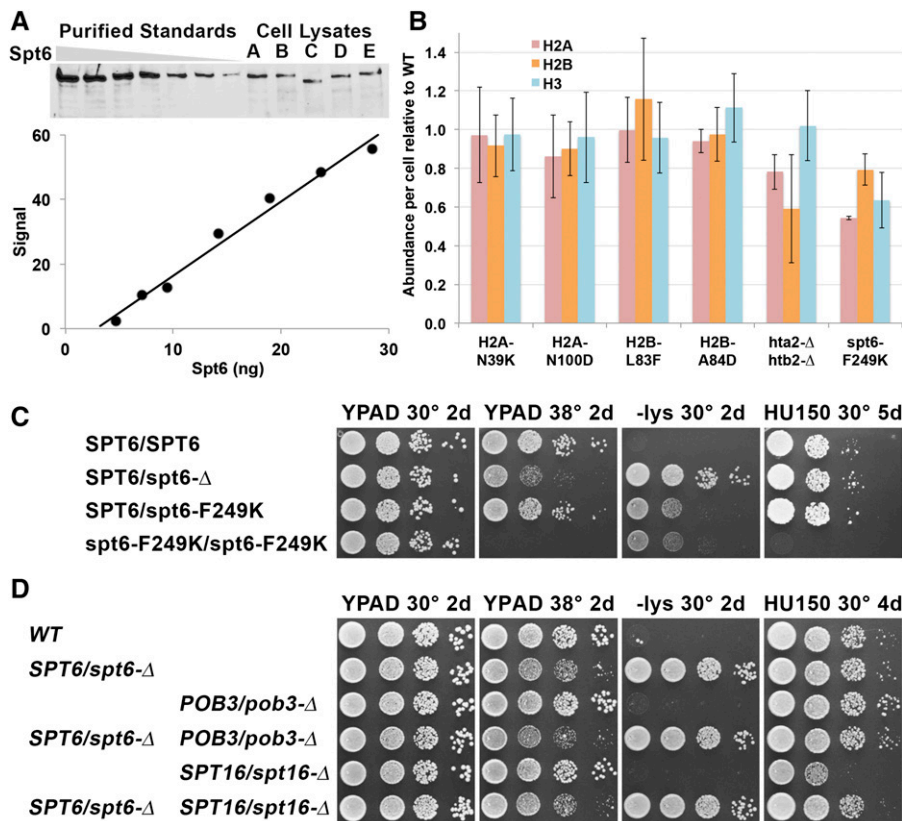
Figure 4 Spt6 is abundant and displays haploinsufficiency. (A) Western blots using polyclonal antiserum against Spt6 were used to detect purified protein or protein extracted from strains A–E (see Table 1; C has the *spt6-50* mutation that lacks the C-terminal domain and therefore produces a shorter protein). Quantitation of the standards is shown below the Western blot; the response was linear in this case but does not pass through the origin, indicating the necessity of using a standard curve to determine an accurate assessment of the amount of Spt6 in the lysates. (B) The amounts of H2A, H2B, and H3 were tested by Western blotting. In this case, a set of dilutions of lysates from a strain with WT histone genes (with the same genetic markers as the mutation being tested downstream of the genes) was used as a standard, and each histone level was normalized to the WT value. Error bars indicate the standard error of at least four measurements (two biological replicates with at least two Western blots each). (C and D) Diploids with the genotypes shown (Table 1) were tested for phenotypes as in Figure 1.

insertion of two negative charges should have the same effect because this would also lead to destabilization of the interface. Similarly, a small uncharged side chain should have less effect. To test this, we constructed strains expressing only H2A-N39D or H2A-N39A from both genomic *HTA* loci and compared their effects on *spt6-F249K* with those of H2A-N39K (Figure 3C). H2A-N39A caused very mild suppression of *spt6-F249K* phenotypes (with the strongest effect on the HUs phenotype), but H2A-N39D was at least as effective a suppressor as H2A-N39K. This result strongly suggests that charge repulsion at the H2A:H2A interface is the feature that is beneficial in *spt6-F249K* strains and that destabilization at this site is likely to be the mechanism of suppression.

The abundance of Spt6 protein

Interactions among histones, histone chaperones, and nucleosomes are likely to be influenced not only by the structures of both partners but also by their binding affinities and concentrations. The abundance of a Spt6-GFP fusion has been estimated to be about 9000 molecules per cell (Ghaemmaghami *et al.* 2003), similar to other histone chaperones such as Asf1 (6200 per cell) and Nap1 (8100 per cell). Estimates for the abundance of FACT vary, ranging from about 10,000 to 50,000 copies per cell, with our previous data giving a value of about 25,000 copies per cell (VanDemark *et al.* 2008). DNA replication requires construction of about 75,000 new nucleosomes during S phase, with about 150,000 molecules of each histone being synthesized, shuttled to replication forks, and assembled. These processes are carefully regulated

because excess histones are detrimental (Meeks-Wagner and Hartwell 1986), and the pool of soluble histone proteins that is not associated with chromatin is small (we previously estimated the free pool of H3 to be about 0.6% of the total H3 in an asynchronous culture) (McCullough *et al.* 2013). Given the potential importance of concentration in understanding the effects of chaperone and histone mutations, we next investigated the abundance of these factors.

We used quantitative Western blots calibrated with purified proteins to measure the abundance of Spt6, FACT, H2A, H2B, and H3 in normal and mutant cells. Western blots were especially challenging with histones because experimental variation was high, dose-response curves were typically nonlinear, and H3 was selectively lost from purified standards with time after preparation of serial dilutions (not shown). Multiple purified controls were required on each gel to ensure that each measurement was flanked by standards and to determine the shape of the dose-response curve. Some of the data for determining the concentration of Spt6 are shown in Figure 4A, and the results of the measurements of protein levels are shown in Table 2, Table 3, and Figure 4B. Errors that would have resulted from using single-point standards and assuming linearity of dose responses would have been significant, necessitating this more rigorous approach.

We found that normal haploid yeast cells contained ~24,000 molecules of Spt6 and ~42,000 copies of FACT (a value for FACT ~70% higher than our previous estimate, which was obtained using a less efficient extraction method) (see *Materials and Methods* and Table 2). Importantly, the
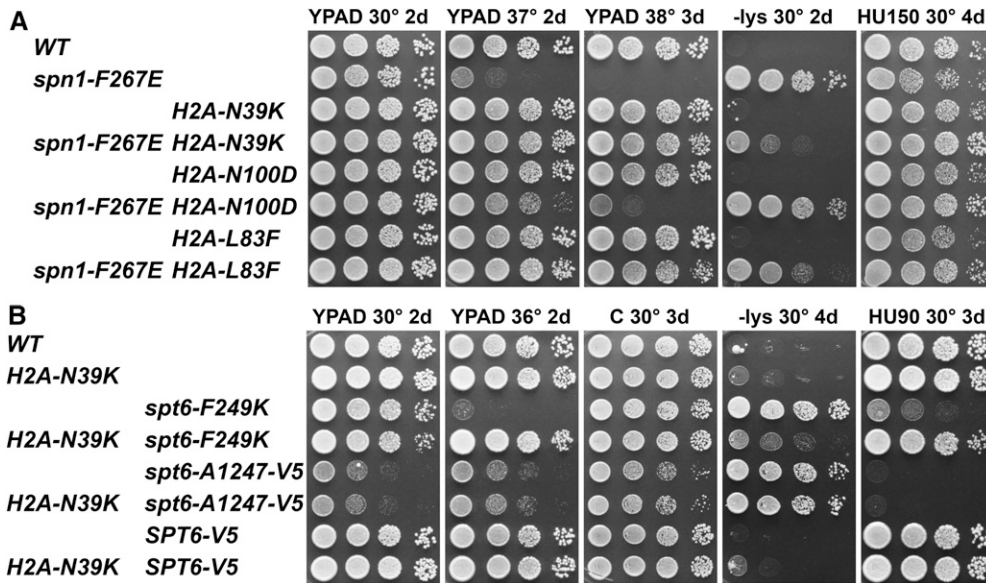
Figure 5 Effects of histone mutations on a *spn1* allele and on other alleles of *spt6*. Strains with the relevant genotypes listed (Table 1) were tested for phenotypes with integrated histone mutations as in Figure 1.

spt6-F249K mutation had little effect on Spt6 abundance or stability at elevated temperatures, unlike the less stable *spt6-14* allele (Table 3). The Ts⁻ phenotype of these strains therefore does not appear to be due to a decrease in protein abundance but rather to a defect in an activity whose importance increases with temperature or that becomes more difficult to perform at higher temperatures. With roughly one molecule of Spt6 per three nucleosomes, each nucleosome is expected to make frequent contact with Spt6. As a test of the importance of this high level of Spt6 activity, we constructed a diploid strain with a single copy of *SPT6* and found that it displayed the Spt⁻ phenotype and a slight growth defect at 38° (but no sensitivity to HU) (Figure 4C). These defects were partially suppressed even by providing more Spt6 in the form of the mutant *spt6-F249K* allele, indicating that high levels of Spt6 are important, especially for maintaining transcriptional repression. Neither *SPT16* nor *POB3* displayed similar haploinsufficiency (Figure 4D) (McCullough *et al.* 2013), suggesting a lower requirement for full levels of FACT or a mechanism for compensating for decreased gene copy number.

The defects caused by FACT mutations can be either enhanced or suppressed by altering histone gene copy number (Formosa *et al.* 2002), raising the possibility that mutations in histone genes cause suppression of *spt6-F249K* not by altering the properties of histones but by changing their stability. We therefore tested a subset of suppressor mutants, but none significantly altered the level of histone proteins (Figure 4B). Notably, deletion of the *HTA2-HTB2* locus caused decreased H2A-H2B levels (but only mild suppression of the HUs phenotype and no effect on the Ts⁻ or Spt⁻ phenotype) (Figure S2), and *spt6-F249K* reduced the concentration of all three histones tested, consistent with the overall loss of transcriptional repression in these strains. The altered properties of the histone mutants and not their stability therefore account for the suppression observed.

The *spt6-F249K* mutation was designed to disrupt the interface between Spt6 and Spn1 (McDonald *et al.* 2010). If weakening of this interaction is the defect whose effects are suppressed by histone mutations, then these histone mutations also should suppress phenotypes caused by other mutations that weaken the interaction. We tested this by examining the effects of suppressors on *spn1-F267E*, a mutation that also weakens the Spt6:Spn1 interface. Indeed, we observed partial suppression of the Ts⁻ and Spt⁻ phenotypes using integrated histone mutations, especially with H2A-N39K, the strongest suppressor of *spt6-F249K* (Figure 5A). These results support the model that Spn1 competition with nucleosomes or histones is a central function of Spt6[239–258].

To determine whether the suppression of *spt6-F249K* by histone mutations is a general property of *spt6* mutants, we combined H2A-N39K with alleles that perturb other domains of Spt6. The *spt6-1004* (Δ931–994) (Kaplan *et al.* 2003) and *spt6-14* (S952F) (Simchen *et al.* 1984 and Fred Winston, personal communication) alleles alter the central core of Spt6 (Johnson *et al.* 2008), and *spt6-50* (K1274stop) (Simchen *et al.* 1984 and Fred Winston, personal communication) and *spt6-A1247-V5* (a precise truncation of the tandem SH2 domain replaced by a V5 epitope) disrupt the C-terminal domain. Each allele causes the Spt⁻ phenotype, the core mutations cause temperature sensitivity, and the C-terminal truncations cause HUs, but none of these phenotypes were significantly affected by H2A-N39K (Figure 5B and Figure S3). The suppression of *spt6-F249K* by this histone mutation is therefore at least partly specific to this allele.

Spt6 binds H2A-H2B and H3-H4

Previous studies showed that immobilized GST-Spt6 retained human or yeast H3-H4 and also human H2A-H2B (Bortvin and Winston 1996). No yeast H2A-H2B interaction was observed, and the human H2A-H2B was released in lower-salt washes than H3-H4. Even though this experiment also showed a potential for H2A-H2B binding, Spt6 subsequently has been broadly considered to be an H3-H4 chaperone (Das and Tyler 2012; Kwak and Lis 2013). Given the prevalence of
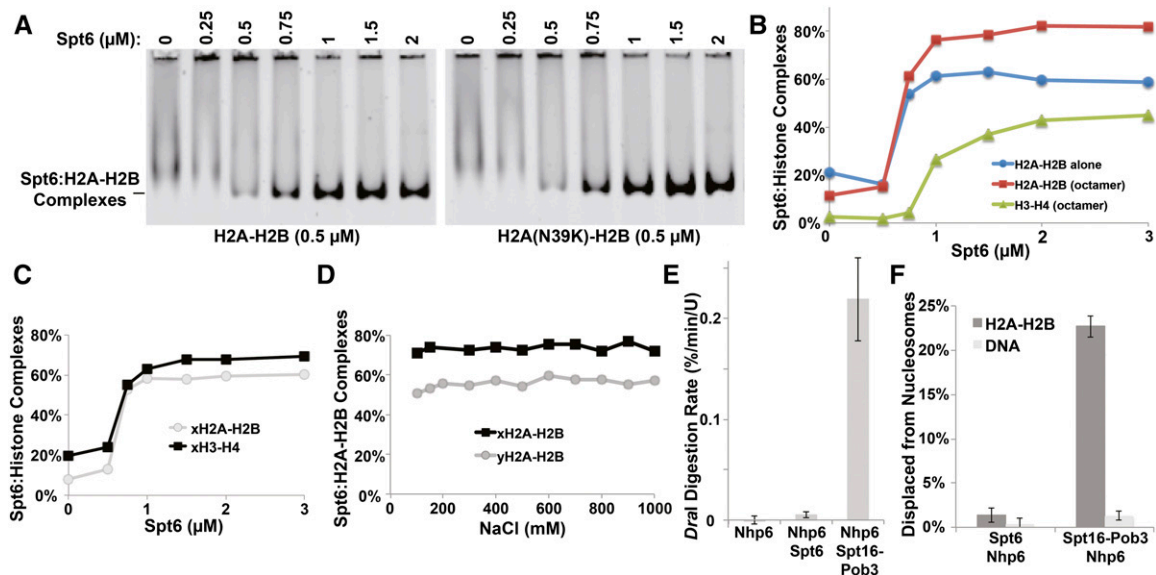
Figure 6 Biochemical analysis of Spt6 functions *in vitro*. (A) Various concentrations of purified Spt6 were mixed with 200 nM yeast H2A or H2A-N39K dimerized with fluorescently labeled H2B. Complexes were separated by native PAGE (EMSA) and detected with a STORM scanner (GE). (B) Complexes were detected as in A but using either H2A-H2B dimers alone or histones assembled into octamers in high salt and then diluted to reaction conditions shortly before use. Signals were plotted for each component as shown. (C) Complexes were detected by EMSA as in A but using labeled recombinant histones with sequences from *X. laevis*. (D) Spt6:H2A-H2B complexes were formed using either yeast or frog proteins and then titrated with NaCl and tested by EMSA. (E) Nucleosomes assembled with 5S rDNA and yeast histones was mixed with Nhp6, Spt6 + Nhp6, or Spt16 − Pob3 and Nhp6 (FACT), and then the rate of digestion of the unique *Dra*I site near the center of the 5S rDNA nucleosome positioning sequence was determined as described by Xin *et al.* (2009). Measurements were made in triplicate, and the average and SD were plotted. (F) Nucleosomes assembled with 5S rDNA and yeast histones with a fluorescent label in the H2A-H2B dimer were incubated with Spt6 + Nhp6 or FACT; then an excess of unlabeled genomic DNA was added prior to electrophoretic separation on native acrylamide gels to disrupt binding to nucleosomes. The amount of H2A-H2B displaced from the nucleosomes was determined in triplicate, and the average and SD were plotted.

H2A-H2B mutations obtained as suppressors of a *spt6* mutation and the overlap with suppressors of defects in FACT, which binds both H3-H4 and H2A-H2B (Winkler *et al.* 2011; Hondele *et al.* 2013; Kemble *et al.* 2013), we revisited the binding of purified Spt6 with histones using a soluble assay instead of the immobilized pull-down approach.

Labeled yeast H2A-H2B dimers do not enter native polyacrylamide gels under our normal electrophoresis conditions, but titration with Spt6 produced stable complexes (Figure 6A). The binding was saturable, displaying half-maximal complex formation at about 700 nM Spt6 (Figure 6, A and B). Similar affinity was observed using dimers containing the H2A-N39K mutation that produced the strongest suppression earlier, indicating that this mutation does not disturb a recognition site for Spt6 (Figure 6A).

Yeast H3-H4 complexes are difficult to test in this assay because they are sparingly soluble under these low-ionic-strength conditions. We therefore used better-behaved histone octamers as the source of histones with different fluorescent labels on H2A and H4. H2A-H2B supplied from octamers displayed the same affinity for Spt6 as when it was supplied as free dimers, and binding to H3-H4 was observed, as expected, with half-maximal binding near 1 μM (Figure 6B). Similar results were obtained with recombinant histones derived from *Xenopus laevis*; in this case, free H3-H4 is soluble, and half-maximal binding was observed at about 600 nM for

both histone complexes (Figure 6C). The Spt6:human H2A-H2B interaction was reported to be more salt sensitive than the H3-H4 interaction (Bortvin and Winston 1996), but we found the complexes with either yeast or frog H2A-H2B to be stable over a broad range of salt concentrations (Figure 6D). This suggests that the binding includes a hydrophobic component and is not simply a result of nonspecific interaction between the acidic N-terminal domain of Spt6 and the basic histones. We conclude that Spt6 can bind both H2A-H2B and H3-H4 with similar affinity in these solution-based binding assays. Together with the previous demonstration that Spt6 can bind DNA and nucleosomes (McDonald *et al.* 2010; Close *et al.* 2011), this makes Spt6 a multifunctional chaperone capable of binding each of the components of the nucleosome as well as the assembled product.

FACT also binds to each component of the nucleosome, with affinity for H3-H4 similar to that observed here but higher affinity for H2A-H2B (about 600 and 30 nM, respectively) (Winkler *et al.* 2011; Hondele *et al.* 2013; Kemble *et al.* 2013). If interaction with each component of the nucleosome is sufficient to produce reorganization, Spt6 also should have this activity. However, Spt6 did not produce either enhanced restriction endonuclease digestion of nucleosomal DNA (Figure 6E) or increased displacement of H2A-H2B dimers (Figure 6F). We conclude that Spt6 and FACT have overlapping activities in terms of binding to nucleosomes and their

Table 1 Strains used

Figure 1	W303 background
8857-13-1	MAT**a** ade2 can1 his3 leu2 lys2-128∂ trp1 ura3 spt6-F249K hht1-hhf1-Δ(::HIS3) hht2-hhf2-Δ(::KanMX) hta1-htb1-Δ(::NatMX) hta2-htb2-Δ(::HphMX) pTF237 (YCp URA3 HHT2-HHF2, HTA1-HTB1)

Figure S1	W303 background
9029-3-2	MAT**a** ade2 can1 his3 leu2 lys2-128∂ met15 trp1 ura3 spt16-11 hht1-hhf1-Δ(::HIS3) hht2-hhf2-Δ(::KanMX3) hta1-htb1-Δ(::NatMX) hta2-htb2-Δ(::HphMX) pTF237 (YCp URA3 HHT2-HHF2, HTA1-HTB1)
9028-6-1	MAT**a** ade2 can1 his3 leu2 lys2-128∂ trp1 ura3 hht1-hhf1-Δ(::HIS3) hht2-hhf2-Δ(::KanMX3) hta1-htb1-Δ(::NatMX) hta2-htb2-Δ(::HphMX) pTF237 (YCp URA3 HHT2-HHF2, HTA1-HTB1)
9028-1-4	MAT**a** ade2 can1 his3 leu2 lys2-128∂ trp1 ura3 pob3-Q308K hht1-hhf1-Δ(::HIS3) hht2-hhf2-Δ(::KanMX3) hta1-htb1-Δ(::NatMX) hta2-htb2-Δ(::HphMX) pTF237 (YCp URA3 HHT2-HHF2, HTA1-HTB1)

Figure 3A	A364a background
8127-7-4	MAT**a** ura3-Δ0 leu2-Δ0 trp1-Δ2 his3 lys2-128∂
9506-1-3	MAT**a** ura3-Δ0 leu2-Δ0 trp1-Δ2 his3 lys2-128∂ spt6-F249K(-424, KanMX)
9008-2-2	MAT**a** ura3-Δ0 leu2-Δ0 trp1-Δ2 his3 lys2-128∂ hta1-N39K(+220, His3MX) hta2-N39K(+30, URA3)
9022-6-2	MATα ura3-Δ0 leu2-Δ0 trp1-Δ2 his3 lys2-128∂ spt6-F249K(-424, KanMX) hta1-N39K(+220, His3MX) hta2-N39K(+30, URA3)
9021-2-4	MAT**a** ura3-Δ0 leu2-Δ0 trp1-Δ2 his3 lys2-128∂ hta1-N100D(+220, His3MX) hta2-N100D(+30, URA3)
9034-3-1	MATα ura3-Δ0 leu2-Δ0 trp1-Δ2 his3 lys2-128∂ spt6-F249K(-424, KanMX) hta1-N100D(+220, His3MX) hta2-N100D(+30, URA3)
8523-2-1	MAT**a** ura3-Δ0 leu2-Δ0 trp1-Δ2 his3 lys2-128∂ hta1-V101I(+220, His3MX) hta2-V101I(+30, URA3)
9636-9-3	MAT**a** ura3-Δ0 leu2-Δ0 trp1-Δ2 his3 lys2-128∂ hta1-V101I(+220, His3MX) hta2-V101I(+30, URA3) spt6-F249K(-424, KanMX)
9019-1-2	MAT**a** ura3-Δ0 leu2-Δ0 trp1-Δ2 his3 lys2-128∂ htb1-L83F(+30, URA3) htb2-L83F(+30, His3MX)
9030-5-4	MAT**a** ura3-Δ0 leu2-Δ0 trp1-Δ2 his3 lys2-128∂ htb1-L83F(+30, URA3) htb2-L83F(+30, His3MX) spt6-F249K(-424, KanMX)
8984-L	MAT**a** ura3-Δ0 leu2-Δ0 trp1-Δ2 his3 lys2-128∂ htb1-A84D(+30, LEU2) htb2-A84D(+30, His3MX)
9487-1-3	MAT**a** ura3-Δ0 leu2-Δ0 trp1-Δ2 his3 lys2-128∂ htb1-A84D(+30, LEU2) htb2-A84D(+30, His3MX) spt6-F249K(-424, URA3)

Figure 3B	A364a background
8127-7-4	MAT**a** ura3-Δ0 leu2-Δ0 trp1-Δ2 his3 lys2-128∂
9659-10-3	MATα ura3-Δ0 leu2-Δ0 trp1-Δ2 his3 lys2-128∂ spt6-F249K(-424, KanMX)
9659-6-4	MATα ura3-Δ0 leu2-Δ0 trp1-Δ2 his3 lys2-128∂ spt6-F249K(-424, KanMX) hta1-N39K(+220, His3MX)
9659-7-3	MATα ura3-Δ0 leu2-Δ0 trp1-Δ2 his3 lys2-128∂ spt6-F249K(-424, KanMX) hta2-N39K(+30, URA3)
9659-7-4	MATα ura3-Δ0 leu2-Δ0 trp1-Δ2 his3 lys2-128∂ spt6-F249K(-424, KanMX) hta1-N39K(+220, His3MX) hta2-N39K(+30, URA3)

Figure 3C	A364a background
8127-7-4	MAT**a** ura3-Δ0 leu2-Δ0 trp1-Δ2 his3 lys2-128∂
9506-1-3	MAT**a** ura3-Δ0 leu2-Δ0 trp1-Δ2 his3 lys2-128∂ spt6-F249K(-424, KanMX)
9008-2-2	MAT**a** ura3-Δ0 leu2-Δ0 trp1-Δ2 his3 lys2-128∂ hta1-N39K(+220, His3MX) hta2-N39K(+30, URA3)
9659-8-3	MAT**a** ura3-Δ0 leu2-Δ0 trp1-Δ2 his3 lys2-128∂ spt6-F249K(-424, KanMX) hta1-N39K(+220, His3MX) hta2-N39K(+30, URA3)
9705-1-2	MAT**a** ura3-Δ0 leu2-Δ0 trp1-Δ2 his3 lys2-128∂ hta1-N39A(+220, His3MX) hta2-N39A(+30, URA3)
9712-8-4	MAT**a** ura3-Δ0 leu2-Δ0 trp1-Δ2 his3 lys2-128∂ hta1-N39A(+220, His3MX) hta2-N39A(+30, URA3) spt6-F249K(-424, KanMX)
9709-5-1	MAT**a** ura3-Δ0 leu2-Δ0 trp1-Δ2 his3 lys2-128∂ hta1-N39D(+220, His3MX) hta2-N39D(+30, URA3)
9713-1-4	MAT**a** ura3-Δ0 leu2-Δ0 trp1-Δ2 his3 lys2-128∂ hta1-N39D(+220, His3MX) hta2-N39D(+30, URA3) spt6-F249K(-424, KanMX)

Figure 4A	Strains for Spt6 abundance measurement (S288c background)
8205-3-1	MAT**a** ura3-52 leu2-Δ1 trp1-Δ63 his4-912∂ lys2-128∂
8142-8-1	MAT**a** ura3-52 leu2-Δ1 his4-912∂ lys2 spt6-14
8164-3-3	MAT**a** ura3-52 leu2-Δ1 trp1-Δ63 his4-912∂ lys2-128∂ spt6-50
8205-5-3	MAT**a** ura3-52 leu2-Δ1 trp1-Δ63 his4-912∂ lys2-128∂ FLAG-spt6-1004
8789-1-3	MAT**a** ura3-52 leu2-Δ1 trp1-Δ63 his4-912∂ lys2-128∂ spt6-F249K(-424, URA3)

Figure 4B	Strains for histone abundance measurement (A364a background)
8500-10-2	MAT**a** ura3-Δ0 leu2-Δ0 trp1-Δ2 his3 lys2-128∂ HTA1(+220, His3MX) HTA2(+30, URA3)
8483-9-1	MAT**a** ura3-Δ0 leu2-Δ0 trp1-Δ2 his3 lys2-128∂ HTB1(+30, URA3) HTB2(+30, His3MX)
9008-2-2	MAT**a** ura3-Δ0 leu2-Δ0 trp1-Δ2 his3 lys2-128∂ hta1-N39K(+220, His3MX) hta2-N39K(+30, URA3)
9021-2-4	MAT**a** ura3-Δ0 leu2-Δ0 trp1-Δ2 his3 lys2-128∂ hta1-N100D(+220, His3MX) hta2-N100D(+30, URA3)
9019-1-2	MAT**a** ura3-Δ0 leu2-Δ0 trp1-Δ2 his3 lys2-128∂ htb1-L83F(+30, URA3) htb2-L83F(+30, His3MX)
8442-4-3	MAT**a** ura3-Δ0 leu2-Δ0 trp1-Δ2 his3 lys2-128∂ htb1-A84D(+30, URA3) htb2-A84D(+30, His3MX)
9430-2-1	ura3-Δ0 leu2-Δ0 trp1-Δ2 his3 lys2-128∂ hta2-htb2-Δ(::HphMX)
9506-1-3	MAT**a** ura3-Δ0 leu2-Δ0 trp1-Δ2 his3 lys2-128∂ spt6-F249K(-424, KanMX)

Table 1, *continued*

Figure 4C	Diploids (A364a background)
8274	*MATa/MATα ura3-Δ0/ura3-Δ0 leu2-Δ0/leu2-Δ0 trp1-Δ2/trp1-Δ2 his3/+ +/his7 lys2-128∂/lys2-128∂*
8537-1	*MATa/MATα ura3-Δ0/ura3-Δ0 leu2-Δ0/leu2-Δ0 trp1-Δ2/trp1-Δ2 his3/+ +/his7 lys2-128∂/lys2-128∂ spt6-Δ(::KanMX)/SPT6*
9465	*MATa/MATα ura3-Δ0/ura3-Δ0 leu2-Δ0/leu2-Δ0 trp1-Δ2/trp1-Δ2 his3/+ +/his7 lys2-128∂/lys2-128∂ spt6-F249K(URA3, -424)/SPT6*
9562	*MATa/MATα ura3-Δ0/ura3-Δ0 leu2-Δ0/leu2-Δ0 trp1-Δ2/trp1-Δ2 his3/+ +/his7 lys2-128∂/lys2-128∂ spt6-F249K(-424, URA3)/spt6-F249K(-424, URA3)*

Figure 4D	Diploids (A364a background)
8274	*MATa/MATα ura3-Δ0/ura3-Δ0 leu2-Δ0/leu2-Δ0 trp1-Δ2/trp1-Δ2 his3/+ +/his7 lys2-128∂/lys2-128∂*
9582	*MATa/MATα ura3-Δ0/ura3-Δ0 leu2-Δ0/leu2-Δ0 trp1-Δ2/trp1-Δ2 his3/+ +/his7 lys2-128∂/lys2-128∂ spt6-Δ(::KanMX)/SPT6*
9191	*MATa/MATα ura3-Δ0/ura3 leu2-Δ0/leu2 trp1-Δ2/trp1 his3/+ +/his7 lys2-128∂/lys2-128∂ pob3-Δ(::LEU2)/POB3*
9649	*MATa/MATα ura3/ura3 leu2/leu2 trp1/trp1 his3/+ +/his7 lys2-128∂/lys2-128∂ spt6-Δ(::KanMX)/SPT6 pob3-Δ2(::LEU2)/POB3*
9650	*MATa/MATα ura3/ura3 leu2-Δ0/leu2 trp1-Δ2/trp1 his3/his3 lys2-128∂/lys2-128∂ spt16-Δ(::HIS3)/SPT16*
9629	*MATa/MATα ura3/ura3 leu2-Δ0/leu2 trp1-Δ2/trp1 his3/his3 lys2-128∂/lys2-128∂ spt6-Δ(::KanMX)/SPT6 spt16-Δ(::HIS3)/SPT16*

Figure 5A	A364a background
8127-7-4	*MATa ura3-Δ0 leu2-Δ0 trp1-Δ2 his3 lys2-128∂*
8824-1-2	*MATa ura3-Δ0 leu2-Δ0 trp1-Δ2 his3 lys2-128∂ spn1-F267E(+49, TRP1)*
9008-2-2	*MATa ura3-Δ0 leu2-Δ0 trp1-Δ2 his3 lys2-128∂ hta1-N39K(+220, His3MX) hta2-N39K(+30, URA3)*
9025-4-1	*MATa ura3-Δ0 leu2-Δ0 trp1-Δ2 his3 lys2-128∂ hta1-N39K(+220, His3MX) hta2-N39K(+30, URA3) spn1-F267E(+49, TRP1)*
9021-2-4	*MATa ura3-Δ0 leu2-Δ0 trp1-Δ2 his3 lys2-128∂ hta1-N100D(+220, His3MX) hta2-N100D(+30, URA3)*
9037-2-1	*MATa ura3-Δ0 leu2-Δ0 trp1-Δ2 his3 lys2-128∂ hta1-N100D(+220, His3MX) hta2-N100D(+30, URA3) spn1-F267E(+49, TRP1)*
9019-1-2	*MATa ura3-Δ0 leu2-Δ0 trp1-Δ2 his3 lys2-128∂ htb1-L83F(+30, URA3) htb2-L83F(+30, His3MX)*
9033-2-4	*MATa ura3-Δ0 leu2-Δ0 trp1-Δ2 his3 lys2-128∂ htb1-L83F(+30, URA3) htb2-L83F(+30, His3MX) spn1-F267E(+49, TRP1)*

Figure 5B	A364a background (V5 epitopes were added after Spt6 A1247 or in place of the native stop codon as a control for the tagged truncation.)
8127-7-4	*MATa ura3-Δ0 leu2-Δ0 trp1-Δ2 his3 lys2-128∂*
9008-2-2	*MATa ura3-Δ0 leu2-Δ0 trp1-Δ2 his3 lys2-128∂ hta1-N39K(+220, His3MX) hta2-N39K(+30, URA3)*
9565-8-1	*MATa ura3-Δ0 leu2-Δ0 trp1-Δ2 his3 lys2-128∂ spt6-F249K(-424, HphMX)*
9659-8-3	*MATa ura3-Δ0 leu2-Δ0 trp1-Δ2 his3 lys2-128∂ spt6-F249K(-424, KanMX) hta1-N39K(+220, His3MX) hta2-N39K(+30, URA3)*
9755-1-4	*MATa ura3-Δ0 leu2-Δ0 trp1-Δ2 his3 lys2-128∂ spt6-A1247-V5(KanMX)*
9775-5-4	*MATa ura3-Δ0 leu2-Δ0 trp1-Δ2 his3 lys2-128∂ spt6-A1247-V5(KanMX) hta1-N39K(220, His3MX) hta2-N39K(30, URA3)*
9756-1-2	*MATa ura3-Δ0 leu2-Δ0 trp1-Δ2 his3 lys2-128∂ SPT6-V5(KanMX)*
9776-2-4	*MATa ura3-Δ0 leu2-Δ0 trp1-Δ2 his3 lys2-128∂ SPT6-V5(KanMX) hta1-N39K(220, His3MX) hta2-N39K(30, URA3)*

Figure S2	A364a background
8127-7-4	*MATa ura3-Δ0 leu2-Δ0 trp1-Δ2 his3 lys2-128∂*
9430-2-4	*MATa ura3-Δ0 leu2-Δ0 trp1-Δ2 his3 lys2-128∂ hta2-Δ-htb2-Δ(::HphMX)*
9560-1-3	*MATa ura3-Δ0 leu2-Δ0 trp1-Δ2 his3 lys2-128∂ spt6-F249K(-424, URA3)*
9587-4-3	*MATa ura3-Δ0 leu2-Δ0 trp1-Δ2 his3 lys2-128∂ hta2-Δ-htb2-Δ(::HphMX) spt6-F249K(-424, URA3)*

Figure S3	S288c background
8266-7-5a	*leu2-Δ1 trp1-Δ63 ura3-52 his4-912∂ lys2-128∂*
9710-1-4	*ura3-52 leu2-Δ1 trp1-Δ63 his4-912∂ lys2-128∂ hta1-N39K(+220, NatMX) hta2-N39K(+30, URA3)*
9584-1-2	*ura3 leu2 trp1 his4-912∂ lys2-128∂ FLAG-spt6-1004*
9717-5-2	*ura3 leu2 trp1 his4-912∂ lys2-128∂ FLAG-spt6-1004 hta1-N39K(+220, NatMX) hta2-N39K(+30, URA3)*
9583-8-1	*ura3 leu2 trp1 his4-912∂ lys2-128∂ spt6-14*
9714-3-4	*ura3 leu2 trp1 his4-912∂ lys2-128∂ spt6-14 hta1-N39K(+220, NatMX) hta2-N39K(+30, URA3)*
9571-2-4	*ura3 leu2 trp1 his4-912∂ lys2-128∂ spt6-50*
9715-4-3	*ura3 leu2 trp1-Δ63 his4-912∂ lys2-128∂ spt6-50 hta1-N39K(+220, NatMX) hta2-N39K(+30, URA3)*

For Figure 1 and Figure S1A–C, the strain listed was used as the parent for the plasmid swaps that replaced pTF237 (YCp *URA3 HHT2-HHF2, HTA1-HTB1*) with the similar plasmids marked with *LEU2* that carry the histone gene mutations noted in each case.

components, but these two essential histone chaperones have distinct biochemical as well as physiological activities.

Discussion

The *spt6-F249K* mutation weakens the interaction between Spt6 and Spn1, and we show here that the resulting defects in chromatin-mediated repression, growth, and ability to tolerate elevated temperatures or the replication toxin HU can be suppressed by mutations in histones H2A or H2B. The common feature of the suppressing mutations is that they appear to destabilize nucleosomal structure, with disturbance of the H2A:H2A interface between the two H2A-H2B dimers within

Table 2 Protein abundance measurements by quantitative Western blotting

Protein	Copies/cell	Number tested
Spt6	24,000 ± 4,000	19
Spt16	44,000 ± 16,000	28
Pob3	41,000 ± 11,000	29

Various strains with the genotypes shown were tested in multiple experiments and averaged with the standard error shown.

Table 3 Effect of temperature shift on Spt6 stability in Ts⁻ mutants

Spt6 allele	Signal at 30°	Signal after 3 hr at 37°	Retention at 37°
WT Spt6	100%	96 ± 6.6%	96%
Spt6-14	82 ± 32%	21 ± 12%	25%
Spt6-50	77 ± 15%	97 ± 24%	125%
Spt6-1004	40 ± 27%	24 ± 1.1%	60%
Spt6-F249K	71 ± 30%	81 ± 11%	115%

The same strains as in Figure 4A were tested under the conditions listed; signals were normalized to Spt6 WT at 30°; experiments were performed in triplicate with the standard error shown.

a nucleosome being especially beneficial. Histone mutations could cause many types of indirect effects, but the cosuppression of *spn1-F267E*, which maps to and weakens the same interface as *spt6-F249K*, by the same histone mutations strongly suggests that the mechanism of suppression centers on the Spt6:Spn1 interaction. A simple explanation for the suppression therefore would be that the histone mutations map the site of interaction between Spt6 and nucleosomes. Spn1 competes with nucleosomes for binding to Spt6, so the balance between these two ligands for occupancy of Spt6 could be a switch that regulates some feature of chromatin maintenance (McDonald *et al.* 2010). Weaker binding of Spt6 to Spn1 then could be compensated by weaker binding of Spt6 to nucleosomes with defective Spt6 interaction sites. Spt6 is usually considered to be an H3-H4 chaperone, which would make it puzzling that our results map putative binding site residues exclusively in H2A-H2B, but Spt6 also binds H2A-H2B (Bortvin and Winston 1996), and we show that this affinity is equivalent to the binding of H3-H4 (Figure 6). However, the broad spatial distribution and inaccessibility of the residues affected by suppressor mutations in the assembled nucleosome (Figure 2) argue against the interpretation that the suppressors are all part of a binding site for Spt6. Further, the most common and strongest suppressor isolated in the screen was H2A-N39K, but H2A-N39D was an equally strong suppressor, whereas H2A-N39A was neutral (Figure 3), and the H2A-N39K mutation did not affect the affinity of Spt6 for H2A-H2B *in vitro* (Figure 6A). Given the role of this residue in forming the contact between the two H2A-H2B dimers in a nucleosome, these observations argue that charge repulsion and therefore destabilization of the nucleosome at this site constitute the mechanism of suppression, not loss of a binding epitope.

FACT is proposed to promote a reversible transition between canonical nucleosomes and a reorganized form comprised of the same components but in a more open, accessible form (Formosa 2012). The Spt16-11 mutant protein is inefficient at maintaining this reorganized state, and some of the phenotypes caused by the *spt16-11* allele were suppressed by some of the same H2A-H2B:H3-H4 interface mutants that were identified here as suppressors of *spt6-F249K* (McCullough *et al.* 2011). In the case of *spt16-11*, we interpreted the suppression as indicating that loosening the nucleosome made reorganization easier, reducing the requirement for efficient FACT activity. However, we show here that Spt6 does not produce the changes in nucleosome structure characteristic of FACT-mediated reorganization *in vitro*, so promoting

reorganization is unlikely to be the mechanism of suppression of *spt6-F249K*. The same form of destabilization of nucleosomes therefore can be beneficial for different chaperone mutants for different mechanistic reasons.

Histone chaperones bind surfaces of histones that would otherwise be prone to forming inappropriate nonspecific interactions, but they must release these surfaces in a coordinated manner to allow efficient nucleosome assembly. For example, Asf1 binds a surface of H3 that is not accessible in an assembled nucleosome (Antczak *et al.* 2006; English *et al.* 2006), and FACT and Spt2 compete with nucleosomal DNA for binding to histones (Hsieh *et al.* 2013; Kemble *et al.* 2013; Chen *et al.* 2015). Destabilization of the nucleosome therefore could assist chaperone functions by making their binding sites within existing nucleosomes more accessible, thereby promoting disassembly of nucleosomes. However, reversal of the Spt⁻ phenotype suggests that suppression results from ameliorating a defect in nucleosome assembly, not a defect in disassembly, because promoting assembly is more likely to enhance chromatin-mediated repression of transcription. It is possible that some perturbations of histone:histone interactions within the nucleosome are beneficial to assembly, but this is unlikely to be the case over the broad range of suppressors identified here. Further, while many of the mutations that destabilize internal nucleosomal interactions suppressed both *spt16-11* and *spt6-F249K*, H2A-N39K was specific for the Spt6 defect. Destabilization is therefore not a simple global property, but one with local, spatial specificity with distinct effects on different chaperones. Together these arguments disfavor the idea that suppression of *spt6-F249K* is due to enhanced accessibility of binding sites for Spt6.

We propose instead that nucleosome assembly includes some assessment of the quality of the product and that the interaction between Spn1 and Spt6 is part of this process. Nucleosome assembly is likely to require multiple steps because chaperones release interfaces and new ones are formed in some ordered sequence. If the interaction between Spn1 and Spt6 is part of a system for monitoring the completion of some step in assembly or certifying the ultimate maturity of the nucleosome, then weakening this interaction could cause the failure of some step to go unnoticed, decreasing the quality of the resulting chromatin. Histones mutations that destabilize internal features of nucleosomes might then suppress this defect by triggering independent monitoring systems, decreasing the importance of

the Spn1:Spt6-mediated process. For example, H2A-N39K might create a strong signal that the H2A:H2A interface is abnormal, and this could either enhance the activity of Spt6 to overcome the barrier or recruit assistance from other assembly factors. In either case, the monitoring function assisted by Spn1 would become less necessary because activation of an alternative sensing system leads to correction of the abnormality. While speculative, this model explains how the broad range of perturbations of internal surfaces suppresses the spt6-F249K allele. It also suggests that different spatial regions of the nucleosome are monitored independently and that quality assessment and nucleosome repair may be important functions of histone chaperones.

We previously suggested a similar concept to explain the specificity of histone mutations that suppress the pob3-Q308K mutation affecting the small subunit of FACT (McCullough et al. 2013). In that case, suppressor mutations clustered in a region of H4 that makes a tight turn as the N-terminal tail joins the globular domain in the assembled nucleosome but is more extended outside a nucleosomal context, such as in the Asf1:H3-H4 complex (Antczak et al. 2006; English et al. 2006). The Pob3-Q308K protein was unable to release efficiently from nucleosomes in vitro, but this defect was corrected by the H4 mutations, suggesting that this domain of FACT is responsible for monitoring the correct folding of this domain or perhaps for preventing it from becoming extended during reorganization, thereby promoting a discrete step on the pathway to nucleosome assembly. The results presented here extend this idea to Spt6, suggesting that this chaperone also has a prominent role in inspecting the quality of nucleosome assembly as well as promoting it mechanistically.

HUs results from a variety of defects (Hartman and Tippery 2004) but is generally linked to a role in DNA replication because this toxin inhibits the production of replication precursors by ribonucleotide reductase. FACT is linked physically and genetically with DNA replication factors (Formosa 2012), but Spt6 has not been implicated previously in replication. Mutations in other transcription factors such as the PAF1 complex also cause HUs (Betz et al. 2002); the linkage between these processes is currently unclear but may involve several different mechanisms including direct collisions between replication and transcription complexes or the effects of residual RNA:DNA hybrids (e.g., see Herrera-Moyano et al. 2014). Suppression of the Spt⁻ phenotype suggests that histone mutations can promote assembly of high-quality chromatin even when Spt6 is defective. If Spt6 contributes to nucleosome assembly or quality monitoring in a general way, then histone mutations that restore this function also could solve the more general problem, restoring efficient chromatin formation in the contexts of replication and repair as well. The possibility that Spt6 contributes to de novo nucleosome assembly either directly or through a monitoring function is an attractive way to explain our results without proposing a new activity for Spt6.

Our previous results revealed unexpected differences when histone gene mutations were expressed from plasmids or from genomic loci, and this also was observed with suppressors of spt6-F249K. For example, suppression by H2A-N39K varied depending on the source of the mutant protein, with Spt⁻ suppression correlating mostly with hta1-N39K but HUs suppression being linked more closely with hta2-N39K (Figure 3). These results underscore the nonequivalence of the two versions of the histone genes, suggesting different roles for each, especially under specific stress conditions, and they highlight the inadequacy of the commonly used method of testing the effects of histone mutations by supplying them from low-copy plasmids in strains lacking genomic versions. Such strains are viable but cannot be considered to be normal or to recapitulate the full repertoire of the mechanisms of regulation of histone expression.

A haploid yeast cell contains about 75,000 nucleosomes, and our Western blot measurements indicated that Spt6 and FACT together nearly match this number, with ~24,000 molecules of Spt6 and ~42,000 molecules of FACT per haploid cell (Table 2). These high values affect models for how these chaperones interact with one another, with histones, and with nucleosomes. Most notably, they suggest that the importance of "recruiting" these chaperones to specific sites within the genome may be a more minor component of regulating their activity than supposed because Spt6 and FACT together are nearly equimolar with nucleosomes. This high abundance is consistent with the proposed role for these chaperones in nucleosomal quality inspection because each chaperone would interact frequently with every nucleosome in the cell.

The results presented here reveal unexpected overlap between the features of nucleosomes that are important to two essential histone chaperones, Spt6 and FACT, and they indicate complexity in the localized spatial dynamics within a nucleosome. Notably, they suggest a role in nucleosome assembly that is more sophisticated than that implied by calling these factors chaperones because they also act as matchmakers that promote nucleosome assembly. This role may include elements of quality sensing and repair of abnormalities, significantly extending the functions of chaperones beyond simple binding of histones.

Acknowledgments

Literature Cited

Adkins, M. W., and J. K. Tyler, 2006 Transcriptional activators are dispensable for transcription in the absence of Spt6-mediated chromatin reassembly of promoter regions. Mol. Cell 21: 405–416.

Antczak, A. J., T. Tsubota, P. D. Kaufman, and J. M. Berger, 2006   Structure of the yeast histone H3-ASF1 interaction: implications for chaperone mechanism, species-specific interactions, and epigenetics. BMC Struct. Biol. 6: 26.

Ardehali, M. B., J. Yao, K. Adelman, N. J. Fuda, S. J. Petesch et al., 2009   Spt6 enhances the elongation rate of RNA polymerase II in vivo. EMBO J. 28: 1067–1077.

Belotserkovskaya, R., A. Saunders, J. T. Lis, and D. Reinberg, 2004   Transcription through chromatin: understanding a complex FACT. Biochim. Biophys. Acta 1677: 87–99.

Betz, J. L., M. Chang, T. M. Washburn, S. E. Porter, C. L. Mueller et al., 2002   Phenotypic analysis of Paf1/RNA polymerase II complex mutations reveals connections to cell cycle regulation, protein synthesis, and lipid and nucleic acid metabolism. Mol. Genet. Genomics 268: 272–285.

Bortvin, A., and F. Winston, 1996   Evidence that Spt6p controls chromatin structure by a direct interaction with histones. Science 272: 1473–1476.

Bucheli, M. E., and S. Buratowski, 2005   Npl3 is an antagonist of mRNA 3′ end formation by RNA polymerase II. EMBO J. 24: 2150–2160.

Chen, S., A. Rufiange, H. Huang, K. R. Rajashankar, A. Nourani et al., 2015   Structure-function studies of histone H3/H4 tetramer maintenance during transcription by chaperone Spt2. Genes Dev. 29: 1326–1340.

Clark-Adams, C. D., D. Norris, M. A. Osley, J. S. Fassler, and F. Winston, 1988   Changes in histone gene dosage alter transcription in yeast. Genes Dev. 2: 150–159.

Close, D., S. J. Johnson, M. A. Sdano, S. M. McDonald, H. Robinson et al., 2011   Crystal Structures of the S. cerevisiae Spt6 Core and C-Terminal Tandem SH2 Domain. J. Mol. Biol. 408: 697–713.

Compagnone-Post, P. A., and M. A. Osley, 1996   Mutations in the SPT4, SPT5, and SPT6 genes alter transcription of a subset of histone genes in Saccharomyces cerevisiae. Genetics 143: 1543–1554.

Das, C., and J. K. Tyler, 2012   Histone exchange and histone modifications during transcription and aging. Biochim. Biophys. Acta 1819: 332–342.

DeGennaro, C. M., B. H. Alver, S. Marguerat, E. Stepanova, C. P. Davis et al., 2013   Spt6 regulates intragenic and antisense transcription, nucleosome positioning, and histone modifications genome-wide in fission yeast. Mol. Cell. Biol. 33: 4779–4792.

Diebold, M. L., M. Koch, E. Loeliger, V. Cura, F. Winston et al., 2010a   The structure of an Iws1/Spt6 complex reveals an interaction domain conserved in TFIIS, Elongin A and Med26. EMBO J. 29: 3979–3991.

Diebold, M. L., E. Loeliger, M. Koch, F. Winston, J. Cavarelli et al., 2010b   A non-canonical tandem SH2 enables interaction of elongation factor SPT6 with RNA polymerase II. J. Biol Chem. 285: 38389–38391.

Dronamraju, R., and B. D. Strahl, 2013   A feed forward circuit comprising Spt6, Ctk1 and PAF regulates Pol II CTD phosphorylation and transcription elongation. Nucleic Acids Res. 42: 870–871.

Endoh, M., W. Zhu, J. Hasegawa, H. Watanabe, D. K. Kim et al., 2004   Human Spt6 stimulates transcription elongation by RNA polymerase II in vitro. Mol. Cell. Biol. 24: 3324–3336.

English, C. M., M. W. Adkins, J. J. Carson, M. E. Churchill, and J. K. Tyler, 2006   Structural basis for the histone chaperone activity of Asf1. Cell 127: 495–508.

Eriksson, P. R., D. Ganguli, V. Nagarajavel, and D. J. Clark, 2012   Regulation of histone gene expression in budding yeast. Genetics 191: 7–20.

Feser, J., D. Truong, C. Das, J. J. Carson, J. Kieft et al., 2010   Elevated histone expression promotes life span extension. Mol. Cell 39: 724–735.

Formosa, T., 2012   The role of FACT in making and breaking nucleosomes. Biochim. Biophys. Acta 1819: 247–255.

Formosa, T., S. Ruone, M. D. Adams, A. E. Olsen, P. Eriksson et al., 2002   Defects in SPT16 or POB3 (yFACT) in Saccharomyces cerevisiae cause dependence on the Hir/Hpc pathway: polymerase passage may degrade chromatin structure. Genetics 162: 1557–1571.

Ghaemmaghami, S., W. K. Huh, K. Bower, R. W. Howson, A. Belle et al., 2003   Global analysis of protein expression in yeast. Nature 425: 737–741.

Hainer, S. J., J. A. Pruneski, R. D. Mitchell, R. M. Monteverde, and J. A. Martens, 2011   Intergenic transcription causes repression by directing nucleosome assembly. Genes Dev. 25: 29–40.

Hartman, J. L. t., and N. P. Tippery, 2004   Systematic quantification of gene interactions by phenotypic array analysis. Genome Biol. 5: R49.

Hartzog, G. A., T. Wada, H. Handa, and F. Winston, 1998   Evidence that Spt4, Spt5, and Spt6 control transcription elongation by RNA polymerase II in Saccharomyces cerevisiae. Genes Dev. 12: 357–369.

Herrera-Moyano, E., X. Mergui, M. L. Garcia-Rubio, S. Barroso, and A. Aguilera, 2014   The yeast and human FACT chromatin-reorganizing complexes solve R-loop-mediated transcription-replication conflicts. Genes Dev. 28: 735–748.

Hondele, M., T. Stuwe, M. Hassler, F. Halbach, A. Bowman et al., 2013   Structural basis of histone H2A-H2B recognition by the essential chaperone FACT. Nature 499: 111–114.

Hsieh, F. K., O. I. Kulaeva, S. S. Patel, P. N. Dyer, K. Luger et al., 2013   Histone chaperone FACT action during transcription through chromatin by RNA polymerase II. Proc. Natl. Acad. Sci. USA 110: 7654–7659.

Ivanovska, I., P. E. Jacques, O. J. Rando, F. Robert, and F. Winston, 2011   Control of chromatin structure by spt6: different consequences in coding and regulatory regions. Mol. Cell. Biol. 31: 531–541.

Jamai, A., A. Puglisi, and M. Strubin, 2009   Histone chaperone spt16 promotes redeposition of the original H3-H4 histones evicted by elongating RNA polymerase. Mol. Cell 35: 377–383.

Johnson, S. J., D. Close, H. Robinson, I. Vallet-Gely, S. L. Dove et al., 2008   Crystal structure and RNA binding of the Tex protein from Pseudomonas aeruginosa. J. Mol. Biol. 377: 1460–1473.

Kaplan, C. D., M. J. Holland, and F. Winston, 2005   Interaction between transcription elongation factors and mRNA 3′-end formation at the Saccharomyces cerevisiae GAL10-GAL7 locus. J. Biol. Chem. 280: 913–922.

Kaplan, C. D., L. Laprade, and F. Winston, 2003   Transcription elongation factors repress transcription initiation from cryptic sites. Science 301: 1096–1099.

Kato, H., K. Okazaki, T. Iida, J. Nakayama, Y. Murakami et al., 2013a   Spt6 prevents transcription-coupled loss of posttranslationally modified histone H3. Sci. Rep. 3: 2186.

Kato, H., K. Okazaki, and T. Urano, 2013b   Spt6: two fundamentally distinct functions in the regulation of histone modification. Epigenetics 8: 1249–1253.

Kemble, D. J., F. G. Whitby, H. Robinson, L. L. McCullough, T. Formosa et al., 2013   Structure of the Spt16 middle domain reveals functional features of the histone chaperone FACT. J. Biol. Chem. 288: 10188–10194.

Krogan, N. J., M. Kim, S. H. Ahn, G. Zhong, M. S. Kobor et al., 2002   RNA polymerase II elongation factors of Saccharomyces cerevisiae: a targeted proteomics approach. Mol. Cell. Biol. 22: 6979–6992.

Kurat, C. F., J. Recht, E. Radovani, T. Durbic, B. Andrews et al., 2014   Regulation of histone gene transcription in yeast. Cell. Mol. Life Sci. 71: 599–613.

Kwak, H., and J. T. Lis, 2013   Control of transcriptional elongation. Annu. Rev. Genet. 47: 483–508.

Lindstrom, D. L., S. L. Squazzo, N. Muster, T. A. Burckin, K. C. Wachter et al., 2003   Dual roles for Spt5 in pre-mRNA processing

and transcription elongation revealed by identification of Spt5-associated proteins. Mol. Cell. Biol. 23: 1368–1378.

McCullough, L., R. Rawlins, A. E. Olsen, H. Xin, D. J. Stillman *et al.*, 2011 Insight into the mechanism of nucleosome reorganization from histone mutants that suppress defects in the FACT histone chaperone. Genetics 188: 835–846.

McCullough, L., B. Poe, Z. Connell, H. Xin, and T. Formosa, 2013 The FACT histone chaperone guides histone H4 into its nucleosomal conformation in *Saccharomyces cerevisiae*. Genetics 195: 101–113.

McDonald, S. M., D. Close, H. Xin, T. Formosa, and C. P. Hill, 2010 Structure and biological importance of the Spn1-Spt6 interaction, and its regulatory role in nucleosome binding. Mol. Cell 40: 725–735.

Meeks-Wagner, D., and L. H. Hartwell, 1986 Normal stoichiometry of histone dimer sets is necessary for high fidelity of mitotic chromosome transmission. Cell 44: 43–52.

Simchen, G., F. Winston, C. A. Styles, and G. R. Fink, 1984 Ty-mediated gene expression of the LYS2 and HIS4 genes of Saccharomyces cerevisiae is controlled by the same SPT genes. Proc. Natl. Acad. Sci. USA 81: 2431–2434.

Sun, M., L. Lariviere, S. Dengl, A. Mayer, and P. Cramer, 2010 A tandem SH2 domain in transcription elongation factor Spt6 binds the phosphorylated RNA polymerase II CTD. J. Biol. Chem. 285: 1597–1603.

Thebault, P., G. Boutin, W. Bhat, A. Rufiange, J. Martens *et al.*, 2011 Transcription regulation by the noncoding RNA SRG1 requires Spt2-dependent chromatin deposition in the wake of RNA polymerase II. Mol. Cell. Biol. 31: 1288–1300.

VanDemark, A. P., M. Blanksma, E. Ferris, A. Heroux, C. P. Hill *et al.*, 2006 The structure of the yFACT Pob3-M domain, its interaction with the DNA replication factor RPA, and a potential role in nucleosome deposition. Mol. Cell 22: 363–374.

VanDemark, A. P., H. Xin, L. McCullough, R. Rawlins, S. Bentley *et al.*, 2008 Structural and functional analysis of the Spt16p N-terminal domain reveals overlapping roles of yFACT subunits. J. Biol. Chem. 283: 5058–5068.

White, C. L., R. K. Suto, and K. Luger, 2001 Structure of the yeast nucleosome core particle reveals fundamental changes in internucleosome interactions. EMBO J. 20: 5207–5218.

Winkler, D. D., and K. Luger, 2011 The histone chaperone FACT: structural insights and mechanisms for nucleosome reorganization. J. Biol. Chem. 286: 18369–18374.

Winkler, D. D., U. M. Muthurajan, A. R. Hieb, and K. Luger, 2011 The histone chaperone FACT coordinates nucleosome interaction through multiple synergistic binding events. J. Biol. Chem. 286: 41883–41892.

Xin, H., S. Takahata, M. Blanksma, L. McCullough, D. J. Stillman *et al.*, 2009 yFACT induces global accessibility of nucleosomal DNA without H2A-H2B displacement. Mol. Cell 35: 365–376.

Yoh, S. M., H. Cho, L. Pickle, R. M. Evans, and K. A. Jones, 2007 The Spt6 SH2 domain binds Ser2-P RNAPII to direct Iws1-dependent mRNA splicing and export. Genes Dev. 21: 160–174.

Yoh, S. M., J. S. Lucas, and K. A. Jones, 2008 The Iws1:Spt6:CTD complex controls cotranscriptional mRNA biosynthesis and HYPB/Setd2-mediated histone H3K36 methylation. Genes Dev. 22: 3422–3434.

Zhang, L., A. G. Fletcher, V. Cheung, F. Winston, and L. A. Stargell, 2008 Spn1 regulates the recruitment of Spt6 and the Swi/Snf complex during transcriptional activation by RNA polymerase II. Mol. Cell. Biol. 28: 1393–1403.
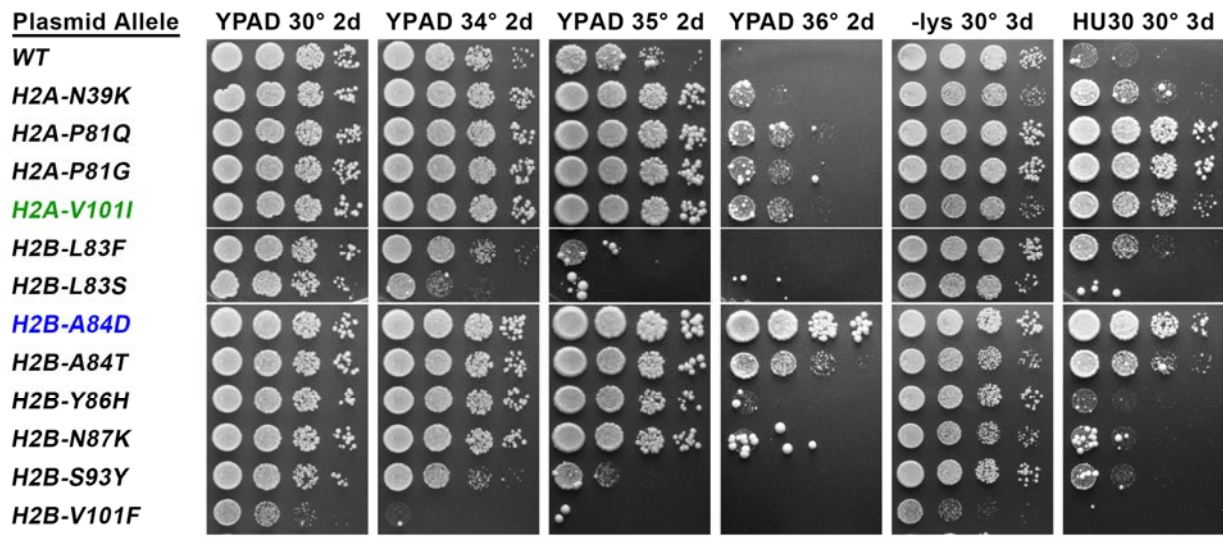
Communicating editor: A. Hinnebusch

GENETICS

The Abundant Histone Chaperones Spt6 and FACT Collaborate to Assemble, Inspect, and Maintain Chromatin Structure in *Saccharomyces cerevisiae*

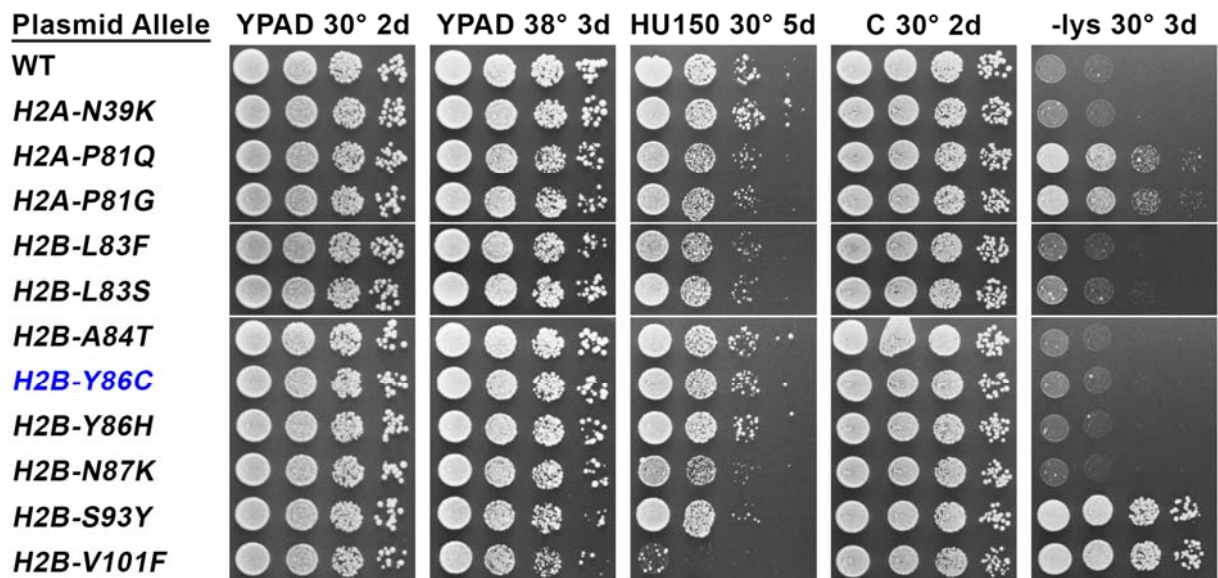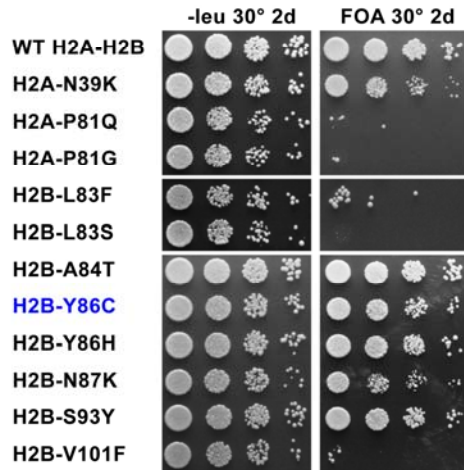Laura McCullough, Zaily Connell, Charisse Petersen, and Tim Formosa

A

spt16-11 histone deletion strain

Plasmid Allele	YPAD 30° 2d	YPAD 34° 2d	YPAD 35° 2d	YPAD 36° 2d	-lys 30° 3d	HU30 30° 3d
WT						
H2A-N39K						
H2A-P81Q						
H2A-P81G						
H2A-V101I						
H2B-L83F						
H2B-L83S						
H2B-A84D						
H2B-A84T						
H2B-Y86H						
H2B-N87K						
H2B-S93Y						
H2B-V101F						

B

WT histone deletion strain

Plasmid Allele	YPAD 30° 2d	YPAD 38° 3d	HU150 30° 5d	C 30° 2d	-lys 30° 3d
WT					
H2A-N39K					
H2A-P81Q					
H2A-P81G					
H2B-L83F					
H2B-L83S					
H2B-A84T					
H2B-Y86C					
H2B-Y86H					
H2B-N87K					
H2B-S93Y					
H2B-V101F					

L. McCullough *et al.*

C

pob3-Q308K histone deletion strain; viability test

pob3-Q308K histone deletion strain; phenotypes of viable combinations
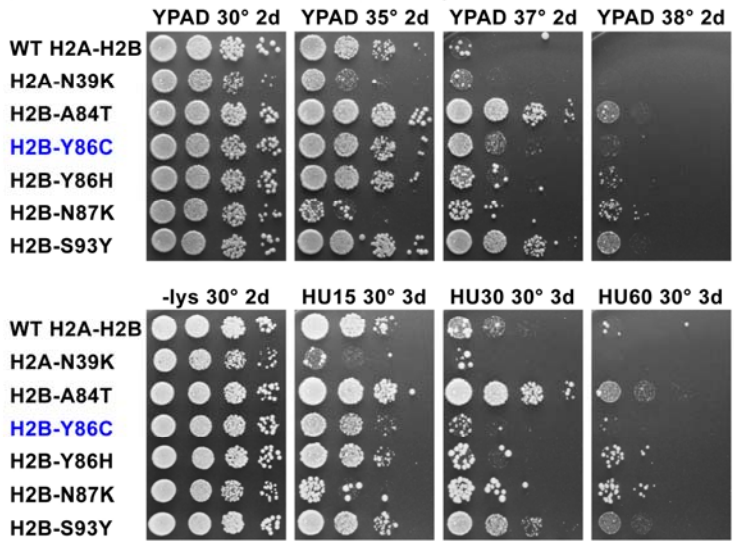
Figure S1

Effects of *spt6-F249K* suppressors in FACT mutants or a WT strain. Tests were conducted as in Fig 1. A) Strain 9029-3-2 pTF237 (*spt16-11* with histone deletions) was transformed with plasmids carrying suppressors of *spt6-F249K* to test for overlap between the two sets of suppressors. B) Strain 9028-6-1 pTF237 (WT with histone deletions) was tested as above to determine the effects of histone mutations in an otherwise normal strain. C) Strain 9028-1-4 pTF237 (*pob3-Q308K* with histone deletions) was tested with the *spt6-F249K* suppressor plasmids and tested as above. Only a subset of the plasmids was able to support growth of the *pob3-Q308K* strain, with others failing to grow on medium containing FOA, indicating inability to lose the WT histone plasmid pTF237 (left panel). Strains that survived this selection were tested for phenotypes as above (right panel).
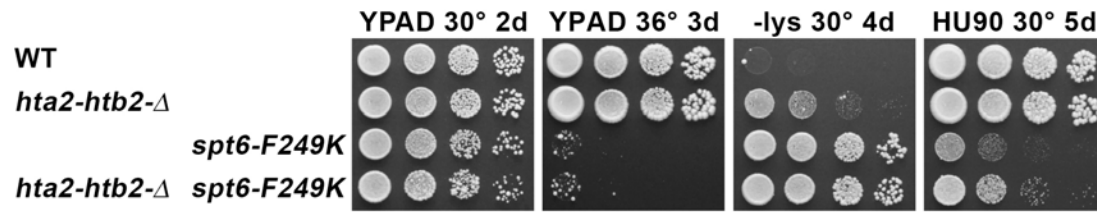
Figure S2
Deletion of *HTA2-HTB2* has mild effects on an *spt6-F249K* strain. Strains with the relevant genotypes listed (Table 1) were tested for phenotypes as in Fig 1.
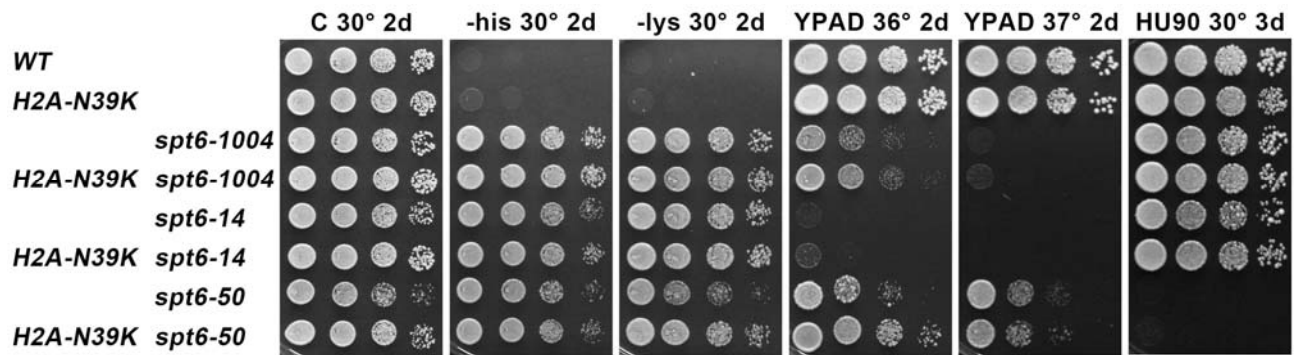
L. McCullough *et al.*

Figure S3

H2A-N39K has minor effects on other alleles of *spt6*. Mutations affecting the central core (*spt6-1004* and *spt6-14*) or C-terminal domain (*spt6-50*) of Spt6 do not show the strong suppression of phenotypes by *hta1-N39K hta2-N39K* that was observed with *spt6-F249K*. Each allele caused a strong Spt⁻ phenotype detected as His⁺ and Lys⁺ phenotypes with these strains that carry both *his4-912∂* and *lys2-128∂* reporters (Table 1). Neither this nor other phenotypes associated with these alleles were strongly suppressed by H2A-N39K.